

Decoupled Crank-Nicolson LeapFrog Methods for the Evolution Boussinesq equations

Xiaofeng Jia¹ and Hui Feng¹

¹Wuhan University

September 8, 2022

Abstract

This paper presents decoupled second-order accurate algorithms based on Crank-Nicolson LeapFrog (CNLF) scheme for the evolution Boussinesq equations. The proposed algorithms deal with the spatial discretization by finite element method and treat the temporal discretization by CNLF method. For the nonlinear term in the Boussinesq equations, the semi-implicit method is used. Unconditional stability and error estimate of the numerical algorithm are proven. Some numerical tests are presented to justify the theoretical analysis.

Decoupled Crank-Nicolson LeapFrog Methods for the Evolution Boussinesq equations

Xiaofeng Jia^a Hui Feng^{a,*}

a School of Mathematics and Statistics, Wuhan University, Wuhan 430072, P.R. China

Abstract This paper presents decoupled second-order accurate algorithms based on Crank-Nicolson LeapFrog (CNLF) scheme for the evolution Boussinesq equations. The proposed algorithms deal with the spatial discretization by finite element method and treat the temporal discretization by CNLF method. For the nonlinear term in the Boussinesq equations, the semi-implicit method is used. Unconditional stability and error estimate of the numerical algorithm are proven. Some numerical tests are presented to justify the theoretical analysis.

Keywords CNLF method; Boussinesq equations; Unconditional stability.

MSC(2000) 35Q30, 74S05

1 Introduction

Let Ω be a bounded domain in $R^d(d = 2, 3)$, with the Lipschitz-continuous boundary Γ . The evolution Boussinesq equations are considered:

$$\begin{cases} \mathbf{u}_t - \nu \Delta \mathbf{u} + (\mathbf{u} \cdot \nabla) \mathbf{u} + \nabla p = -k\nu^2 \mathbf{g}\theta + \mathbf{f} & \text{in } \Omega \times (0, T], \\ \nabla \cdot \mathbf{u} = 0 & \text{in } \Omega \times (0, T], \\ \theta_t - \lambda \nu \Delta \theta + (\mathbf{u} \cdot \nabla) \theta = b & \text{in } \Omega \times (0, T], \\ \mathbf{u}(x, 0) = \mathbf{u}_0, \theta(x, 0) = \theta_0 & \text{in } \Omega, \\ \mathbf{u} = 0, \theta = 0 & \text{on } \Gamma \times (0, T], \end{cases} \quad (1.1)$$

where $\mathbf{u}(x, t)$, \mathbf{f} , $p(x, t)$ represent the flow velocity, the external body force and the pressure, respectively. $T > 0$ represents a finite constant and ν is the kinematic viscosity. θ is the temperature, k is the Grashoff number and $\lambda = Pr^{-1}$, Pr is the Prandtl number. \mathbf{g} represents the vector of gravitational acceleration. b is the temperature source term. When the temperature θ is equal to zero or constant, the evolution Boussinesq equations reduce to the incompressible Navier-Stokes equations.

The evolution Boussinesq equations [1], which model the motion of the incompressible flows with the influence of temperature, can be used to describe many real situations, such as room

The work of this author was supported by National Natural Science Foundation of China (No.91130022, No.10971159 and No.11161130003) and The Doctoral Fund of Ministry of Education of China (No.20130141110026).

*Corresponding Author: hfeng.math@whu.edu.cn

ventilation, the connections between oceanic and atmospheric dynamics and so on. The existence of the solutions for the Boussinesq problem can refer to the literatures [2-3]. Due to the coupling of the velocity, pressure and the temperature among the evolution Boussinesq equations, finding the accurate numerical solution becomes a more difficult task. There were many literatures to study this problem in [4-10].

In recent years, the projection/Lagrange-Galerkin finite element method was studied for the Boussinesq equations in [11]. Two-grid Crank-Nicolson extrapolation scheme was proposed for the time-dependent natural convection equations in [12]. A second-order accurate algorithm was presented for calculating an ensemble of solutions to natural convection problems in [13].

The CNLF method was first analyzed in [14], and stability for the CNLF method was proven in [15]. The CNLF method was used to solve the non-stationary Stokes-Darcy or Navier-Stokes equations in [16-18]. Compared to Crank-Nicolson extrapolation scheme, the CNLF method method is easier to decouple for solving the Boussinesq equations. In the paper, we try to extend the CNLF method to solve the evolution Boussinesq equations.

This paper is organized as follows: Section 2 collects some preliminaries and gives associated weak formulation; In section 3, the decoupled CNLF schemes based on finite element method are given; In section 4, the unconditional stability of the decoupled CNLF method is proved; In section 5, error estimate for the decoupled CNLF method is derived; In section 6, numerical experiments are given to illustrate the theoretical analysis; Finally, the conclusion is obtained.

2 Preliminaries

The space $L^2(\Omega)$, is equipped with L^2 -scalar product (\cdot, \cdot) and L^2 -norm $\|\cdot\|_0$. The following Hilbert spaces(velocity, pressure and temperature) are defined:

$$\begin{aligned} X &:= H_0^1(\Omega)^d = \{\mathbf{v} \in (H^1(\Omega))^d : \mathbf{v} = 0 \text{ on } \Gamma\}, Q := L_0^2(\Omega) = \{q \in (L^2(\Omega)) : \int_{\Omega} q dx = 0\}, \\ V &:= \{\mathbf{v} \in X : (\nabla \cdot \mathbf{v}, q) = 0, \forall q \in Q\}, \quad W := \{\psi \in (H^1(\Omega)) : \psi = 0 \text{ on } \Gamma\}. \end{aligned}$$

The spaces X and W are equipped with the following norms:

$$\begin{aligned} \|\mathbf{u}\|_X &= \|\nabla \mathbf{u}\|_0 = \sqrt{(\nabla \mathbf{u}, \nabla \mathbf{u})_{\Omega}} \quad \forall \mathbf{u} \in X, \\ \|\theta\|_W &= \|\nabla \theta\|_0 = \sqrt{(\nabla \theta, \nabla \theta)_{\Omega}} \quad \forall \theta \in W, \end{aligned}$$

Since the norm equivalence between $\|\mathbf{u}\|_1$, $\|\theta\|_1$ and $\|\nabla \mathbf{u}\|_0$, $\|\nabla \theta\|_0$ on X, W , the same notation is used for them.

For the nonlinear terms in (1.1), the skew-symmetric trilinear forms [4,8] are defined: $\forall \mathbf{u}, \mathbf{v}, \mathbf{w} \in X, \theta, \psi \in W$:

$$\begin{aligned} N(\mathbf{u}; \mathbf{w}, \mathbf{v}) &:= ((\mathbf{u} \cdot \nabla) \mathbf{w}, \mathbf{v}) = \frac{1}{2}(\mathbf{u} \cdot \nabla \mathbf{w}, \mathbf{v}) - \frac{1}{2}(\mathbf{u} \cdot \nabla \mathbf{v}, \mathbf{w}), \\ \bar{N}(\mathbf{u}; \theta, \psi) &:= ((\mathbf{u} \cdot \nabla) \theta, \psi) = \frac{1}{2}(\mathbf{u} \cdot \nabla \theta, \psi) - \frac{1}{2}(\mathbf{u} \cdot \nabla \psi, \theta). \end{aligned}$$

The following equalities and inequalities can be obtained from [7,19,20]:

$$\begin{aligned}
N(\mathbf{u}; \mathbf{v}, \mathbf{v}) &= 0, \quad \forall \mathbf{u}, \mathbf{v} \in X, \quad \bar{N}(\mathbf{u}; \theta, \theta) = 0, \quad \forall \mathbf{u} \in X, \theta \in W \\
|N(\mathbf{u}; \mathbf{w}, \mathbf{v})| &\leq C\|\mathbf{u}\|_1\|\mathbf{w}\|_1\|\mathbf{v}\|_1, \quad \forall \mathbf{u}, \mathbf{w}, \mathbf{v} \in H_0^1(\Omega)^d, \\
|N(\mathbf{u}; \mathbf{w}, \mathbf{v})| &\leq C\|\mathbf{u}\|_2\|\mathbf{w}\|_0\|\mathbf{v}\|_1, \quad \forall \mathbf{u} \in H^2(\Omega)^d \cap H_0^1(\Omega)^d, \mathbf{w}, \mathbf{v} \in H_0^1(\Omega)^d, \\
|N(\mathbf{u}; \mathbf{w}, \mathbf{v})| &\leq C\|\mathbf{u}\|_0\|\mathbf{w}\|_2\|\mathbf{v}\|_1, \quad \forall \mathbf{w} \in H^2(\Omega)^d \cap H_0^1(\Omega)^d, \mathbf{u}, \mathbf{v} \in H_0^1(\Omega)^d. \\
|\bar{N}(\mathbf{u}; \theta, \psi)| &\leq C\|\mathbf{u}\|_1\|\theta\|_1\|\psi\|_1, \quad \forall \mathbf{u} \in X, \theta, \psi \in W \\
|\bar{N}(\mathbf{u}; \theta, \psi)| &\leq C\|\mathbf{u}\|_2\|\theta\|_0\|\psi\|_1, \quad \forall \mathbf{u} \in H^2(\Omega)^d \cap X, \theta, \psi \in W, \\
|\bar{N}(\mathbf{u}; \theta, \psi)| &\leq C\|\mathbf{u}\|_0\|\theta\|_2\|\psi\|_1, \quad \forall \theta \in H^2(\Omega)^d \cap W, \mathbf{u} \in X, \psi \in W
\end{aligned} \tag{2.1}$$

We recall Poincaré inequality that is used in the theoretical analysis. There exist positive constants C_P, \tilde{C}_P which only depend on the domain Ω :

$$\|\mathbf{v}\|_0 \leq C_P\|\mathbf{v}\|_1, \|\theta\|_0 \leq \tilde{C}_P\|\theta\|_1.$$

The weak formulation of the evolution Boussinesq equations is the following: find $(\mathbf{u}, p, \theta) \in (X, Q, W)$, for all $t \in (0, T]$

$$\left\{
\begin{array}{ll}
(\mathbf{u}_t, \mathbf{v}) + a(\mathbf{u}, \mathbf{v}) + \tilde{b}(\mathbf{v}, p) + N(\mathbf{u}; \mathbf{u}, \mathbf{v}) = (-k\nu^2 \mathbf{g}\theta, \mathbf{v}) + (\mathbf{f}, \mathbf{v}) & \forall \mathbf{v} \in X, \\
(\nabla \cdot \mathbf{u}, q) = 0 & \forall q \in Q, \\
(\theta_t, \psi) + c(\theta, \psi) + \bar{N}(\mathbf{u}; \theta, \psi) = (b, \psi), & \forall \psi \in W \\
\mathbf{u}(0) = \mathbf{u}_0, \theta(0) = \theta_0 & \\
a(\mathbf{u}, \mathbf{v}) = \nu(\nabla \mathbf{u}, \nabla \mathbf{v}), \quad \tilde{b}(\mathbf{v}, p) = -(p, \nabla \cdot \mathbf{v}), \quad c(\theta, \psi) = \lambda\nu(\nabla \theta, \nabla \psi). &
\end{array}
\right. \tag{2.2}$$

3 Decoupled CNLF Algorithm

Consider a quasi-uniform triangulation τ_h for the domain Ω with mesh size $0 < h < 1$, either with triangles if $d = 2$ or tetrahedra if $d = 3$. We use the conforming velocity, pressure and temperature finite element subspaces ($X_h \subset X$, $Q_h \subset Q$, $W_h \subset W$) which consist of piecewise continuous polynomials of degree m_1, s , and m_1 , respectively. Velocity and pressure finite element subspaces satisfy the discrete inf-sup condition: there exists a positive constant β , independent of h , such that $\forall q_h \in Q_h$, $\exists \mathbf{v}_h \in X_h$, $\mathbf{v}_h \neq 0$,

$$\tilde{b}(\mathbf{v}_h, q_h) \geq \beta\|\mathbf{v}_h\|_1\|q_h\|_0.$$

In the paper, the well-known Mini mixed finite elements $P_1 b - P_1$ and Taylor-Hood mixed finite elements $P_2 - P_1$ are considered.

In order to introduce the L_2 -orthogonal projection $P_h : L^2(\Omega)^d \rightarrow V_h$, the discretely divergence free subspace of X_h is defined: $V_h := \{\mathbf{v}_h \in X_h : (q_h, \nabla \cdot \mathbf{v}_h) = 0, \forall q_h \in Q_h\}$. We assume that for the finite element subspaces, the following approximation properties in [21] hold: for $(\mathbf{v}, q) \in (H^2(\Omega)^d \cap V, H^1(\Omega) \cap Q)$, there exist approximations $\tilde{\mathbf{v}} \in V_h, \tilde{q} \in Q_h$ such that:

$$\begin{aligned}
\|\tilde{\mathbf{v}}\|_1 &\leq C\|\mathbf{v}\|_1, \quad \|\mathbf{v} - \tilde{\mathbf{v}}\|_0 + h\|\mathbf{v} - \tilde{\mathbf{v}}\|_1 \leq Ch^{m_1+1}\|\mathbf{v}\|_{H^{m_1+1}(\Omega)}, \\
\|q - \tilde{q}\|_0 &\leq Ch^{s_1}\|q\|_{H^{s_1}(\Omega)}.
\end{aligned} \tag{3.1}$$

Lemma 3.1.[11, Lemma 3.7] There exists $r_h : W \rightarrow W_h$ for all $\psi \in W$, $r_h\psi = \tilde{\psi}$, which holds that

$$(\nabla(\psi - \tilde{\psi}), \nabla\psi_h) = 0, \forall \psi_h \in W_h, \|\tilde{\psi}\|_1 \leq C\|\psi\|_1. \quad (3.2)$$

When $\psi \in W^{r,q}(\Omega)$ ($1 \leq q \leq \infty$), there holds

$$\|\psi - \tilde{\psi}\|_{-s,q} \leq Ch^{r+s}|\psi|_{r,q}, -1 \leq s \leq m_1, 0 \leq r \leq m_1 + 1. \quad (3.3)$$

Remark. When the finite element spaces are selected as $P_2 - P_1 - P_2$, $P_{1b} - P_1 - P_1$, respectively, the values of m_1, s_1 are 2, 1, 1, 1.

Assume a uniform distribution of discrete time levels with $t_m = m\Delta t$, $m = 0, 1, 2, \dots, M$ for $\Delta t = \frac{T}{M}$. \mathbf{u}_h^m , p_h^m , θ_h^m denote the discrete approximation solutions for $(\mathbf{u}(t_m), p(t_m), \theta(t_m))$.

Algorithm The decoupled CNLF

Given \mathbf{u}_h^0 , θ_h^0 , find $(\mathbf{u}_h^{m+1}, p_h^m) \in (X_h, Q_h)$, with $m = 1, \dots, M-1$, such that :

$$\begin{aligned} & (\frac{\mathbf{u}_h^{m+1} - \mathbf{u}_h^{m-1}}{2\Delta t}, \mathbf{v}_h) + a(\frac{\mathbf{u}_h^{m+1} + \mathbf{u}_h^{m-1}}{2}, \mathbf{v}_h) + \tilde{b}(\mathbf{v}_h, p_h^m) + N(\mathbf{u}_h^m; \frac{\mathbf{u}_h^{m+1} + \mathbf{u}_h^{m-1}}{2}, \mathbf{v}_h) \\ &= -k\nu^2 \mathbf{g}(\theta_h^m, \mathbf{v}_h) + (\mathbf{f}^m, \mathbf{v}_h), \\ & \tilde{b}(\frac{\mathbf{u}_h^{m+1} + \mathbf{u}_h^{m-1}}{2}, q_h) = 0, \quad \forall (\mathbf{v}_h, q_h) \in (X_h, Q_h) \end{aligned} \quad (3.4)$$

Given θ_h^0 , θ_h^1 , find $\theta_h^{m+1} \in W_h$, with $m = 1, \dots, M-1$, such that :

$$(\frac{\theta_h^{m+1} - \theta_h^{m-1}}{2\Delta t}, \psi_h) + c(\frac{\theta_h^{m+1} + \theta_h^{m-1}}{2}, \psi_h) + \bar{N}(\mathbf{u}_h^m; \frac{\theta_h^{m+1} + \theta_h^{m-1}}{2}, \psi_h) = (b^m, \psi_h), \forall \psi_h \in W_h. \quad (3.5)$$

Remark. Notice that the CNLF schemes are a three level method. The value of initial time $(\mathbf{u}_h^0, \theta_h^0)$ is usually obtained by exact solution. To get the first time value $(\mathbf{u}_h^1, \theta_h^1)$, another numerical method can be used. Note that errors in the first step will affect the overall convergence rate of the CNLF method. In this paper, for the sake of simplicity, the first time value $(\mathbf{u}_h^1, \theta_h^1)$ is also obtained by exact solution. But for some practical problems, the exact solution is unknown, the first time value $(\mathbf{u}_h^1, \theta_h^1)$ can be obtained by Crank-Nicolson linear extrapolation scheme in [8].

4 The Unconditional Stability

In this section, we will prove the stability of the decoupled CNLF algorithm.

Lemma 4.1(Discrete Gronwall Lemma). Let Δt , H , a_n , b_n , c_n , d_n be non-negative numbers for integers $n \geq 0$ such that for $N \geq 1$. If

$$a_N + \Delta t \sum_{n=0}^N b_n \leq \Delta t \sum_{n=0}^{N-1} d_n a_n + \Delta t \sum_{n=0}^N c_n + H$$

then for all $\Delta t > 0$.

$$a_N + \Delta t \sum_{n=0}^N b_n \leq \exp(\Delta t \sum_{n=0}^{N-1}) (\Delta t \sum_{n=0}^N c_n + H).$$

Theorem 4.1(unconditional Stability) Assume that $\mathbf{f} \in L^2(0, T; L^2(\Omega)^d)$, $b \in L^2(0, T; L^2(\Omega))$ and the initial data $\theta_h^0 = \theta_0$, $\mathbf{u}_h^0 = \mathbf{u}_0$, $\theta_h^1 = \theta_1$, $\mathbf{u}_h^1 = \mathbf{u}_1$. For $1 \leq n \leq M - 1$, the solutions of the Algorithm hold:

$$\begin{aligned} & \|\mathbf{u}_h^{n+1}\|_0^2 + \|\mathbf{u}_h^n\|_0^2 + \|\theta_h^{n+1}\|_0^2 + \|\theta_h^n\|_0^2 + \frac{\nu \Delta t}{4} \sum_{m=1}^n \|\mathbf{u}_h^{m+1} + \mathbf{u}_h^{m-1}\|_1^2 + \frac{\lambda \nu \Delta t}{2} \sum_{m=1}^n \|\theta_h^{m+1} + \theta_h^{m-1}\|_1^2 \\ & \leq \hat{C} \left(\frac{2C_P^2 \Delta t}{\nu} \sum_{m=1}^n \|\mathbf{f}^m\|_0^2 + \frac{2\tilde{C}_P^2 \Delta t}{\lambda \nu} \sum_{m=1}^n \|b^m\|_0^2 + \|\mathbf{u}_h^0\|_0^2 + \|\mathbf{u}_h^1\|_0^2 + \|\theta_h^0\|_0^2 + \|\theta_h^1\|_0^2 \right) \end{aligned} \quad (4.1)$$

where the constant $\hat{C} = \exp(\Delta t \sum_{m=1}^n \frac{16C_P^2 k^2 \nu^4 \mathbf{g}^2}{\nu})$.

Proof. Taking $\mathbf{v}_h = \mathbf{u}_h^{m+1} + \mathbf{u}_h^{m-1}$, $q_h = 2p_h^m$ in (3.4) and $\psi_h = \theta_h^{m+1} + \theta_h^{m-1}$ in (3.5), we can obtain:

$$\begin{aligned} & \left(\frac{\mathbf{u}_h^{m+1} - \mathbf{u}_h^{m-1}}{2\Delta t}, \mathbf{u}_h^{m+1} + \mathbf{u}_h^{m-1} \right)_\Omega + a\left(\frac{\mathbf{u}_h^{m+1} + \mathbf{u}_h^{m-1}}{2}, \mathbf{u}_h^{m+1} + \mathbf{u}_h^{m-1} \right) + N(\mathbf{u}_h^m; \frac{\mathbf{u}_h^{m+1} + \mathbf{u}_h^{m-1}}{2}, \mathbf{u}_h^{m+1} + \mathbf{u}_h^{m-1}) \\ & = -k\nu^2 \mathbf{g}(\theta_h^m, \mathbf{u}_h^{m+1} + \mathbf{u}_h^{m-1}) + (\mathbf{f}^m, \mathbf{u}_h^{m+1} + \mathbf{u}_h^{m-1}), \end{aligned} \quad (4.2)$$

$$\begin{aligned} & \left(\frac{\theta_h^{m+1} - \theta_h^{m-1}}{2\Delta t}, \theta_h^{m+1} + \theta_h^{m-1} \right) + c\left(\frac{\theta_h^{m+1} + \theta_h^{m-1}}{2}, \theta_h^{m+1} + \theta_h^{m-1} \right) + \bar{N}(\mathbf{u}_h^m; \frac{\theta_h^{m+1} + \theta_h^{m-1}}{2}, \theta_h^{m+1} + \theta_h^{m-1}) \\ & = (b^m, \theta_h^{m+1} + \theta_h^{m-1}). \end{aligned} \quad (4.3)$$

Adding (4.2) and (4.3), by using the first two equalities in (2.1), we have:

$$\begin{aligned} & \frac{1}{2\Delta t} (\|\mathbf{u}_h^{m+1}\|_0^2 + \|\theta_h^{m+1}\|_0^2 - \|\mathbf{u}_h^{m-1}\|_0^2 - \|\theta_h^{m-1}\|_0^2) + \frac{\nu}{2} \|\mathbf{u}_h^{m+1} + \mathbf{u}_h^{m-1}\|_1^2 + \frac{\lambda \nu}{2} \|\theta_h^{m+1} + \theta_h^{m-1}\|_1^2 \\ & = -k\nu^2 \mathbf{g}(\theta_h^m, \mathbf{u}_h^{m+1} + \mathbf{u}_h^{m-1}) + (\mathbf{f}^m, \mathbf{u}_h^{m+1} + \mathbf{u}_h^{m-1}) + (b^m, \theta_h^{m+1} + \theta_h^{m-1}) \\ & = \sum_{i=1}^3 A_i. \end{aligned} \quad (4.4)$$

For any $\varepsilon > 0$, the A_1 can be estimated by Hölder, Poincaré, and Young inequalities:

$$|A_1| \leq C_P k \nu^2 \mathbf{g} \|\theta^m\|_0 \|\mathbf{u}_h^{m+1} + \mathbf{u}_h^{m-1}\|_1 \leq \frac{C_P^2 k^2 \nu^4 \mathbf{g}^2}{\varepsilon \nu} \|\theta^m\|_0^2 + \varepsilon \nu \|\mathbf{u}_h^{m+1} + \mathbf{u}_h^{m-1}\|_1^2. \quad (4.5)$$

The A_2, A_3 can be estimated by a similar technique:

$$\begin{aligned} |A_2 + A_3| & \leq C_P \|\mathbf{f}^m\|_0 \|\mathbf{u}_h^{m+1} + \mathbf{u}_h^{m-1}\|_1 + \tilde{C}_P \|b^m\|_0 \|\theta_h^{m+1} + \theta_h^{m-1}\|_1 \\ & \leq \frac{C_P^2}{\nu} \|\mathbf{f}^m\|_0^2 + \frac{\nu}{4} \|\mathbf{u}_h^{m+1} + \mathbf{u}_h^{m-1}\|_1^2 + \frac{\tilde{C}_P^2}{\lambda \nu} \|b^m\|_0^2 + \frac{\lambda \nu}{4} \|\theta_h^{m+1} + \theta_h^{m-1}\|_1^2. \end{aligned} \quad (4.6)$$

Substituting (4.5-4.6) into (4.4) and taking $\varepsilon = \frac{1}{8}$, we obtain:

$$\begin{aligned} & \frac{1}{2\Delta t} (\|\mathbf{u}_h^{m+1}\|_0^2 + \|\theta_h^{m+1}\|_0^2 - \|\mathbf{u}_h^{m-1}\|_0^2 - \|\theta_h^{m-1}\|_0^2) + \frac{\nu}{8} \|\mathbf{u}_h^{m+1} + \mathbf{u}_h^{m-1}\|_1^2 + \frac{\lambda \nu}{4} \|\theta_h^{m+1} + \theta_h^{m-1}\|_1^2 \\ & \leq \frac{C_P^2}{\nu} \|\mathbf{f}^m\|_0^2 + \frac{\tilde{C}_P^2}{\lambda \nu} \|b^m\|_0^2 + \frac{8C_P^2 k^2 \nu^4 \mathbf{g}^2}{\nu} \|\theta^m\|_0^2. \end{aligned} \quad (4.7)$$

Multiplying (4.7) by $2\Delta t$, summing the resultant over $m = 1, \dots, n$ and by using Lemma 4.1, we complete the proof. \square

5 The Convergence

To facilitate convergence analysis, we will introduce some notations:

$$\begin{aligned}\mathbf{u}^m &= \mathbf{u}(t_m), \theta^m = \theta(t_m), p^m = p(t_m), \\ \mathbf{e}_1^m &= \mathbf{u}^m - \tilde{\mathbf{u}}^m, \epsilon_1^m = \theta^m - \tilde{\theta}^m, \eta_1^m = p^m - \tilde{p}^m, \\ \mathbf{e}^m &= \tilde{\mathbf{u}}^m - \mathbf{u}_h^m, \epsilon^m = \tilde{\theta}^m - \theta_h^m, \eta^m = \tilde{p}^m - p_h^m, \\ \mathbf{u}^m - \mathbf{u}_h^m &= \mathbf{e}^m + \mathbf{e}_1^m, \theta^m - \theta_h^m = \epsilon^m + \epsilon_1^m, p^m - p_h^m = \eta^m + \eta_1^m.\end{aligned}$$

Lemma 5.1. The following inequalities hold:

$$\begin{aligned}\Delta t \sum_{m=1}^n \|\mathbf{u}_t^m - \frac{\mathbf{u}^{m+1} - \mathbf{u}^{m-1}}{2}\|_0^2 &\leq \frac{\Delta t^4}{20} \|\mathbf{u}_{ttt}\|_{L^2(0,T;L^2(\Omega))}^2 \\ \Delta t \sum_{m=1}^n \|\theta_t^m - \frac{\theta^{m+1} - \theta^{m-1}}{2}\|_0^2 &\leq \frac{\Delta t^4}{20} \|\theta_{ttt}\|_{L^2(0,T;L^2(\Omega))}^2 \\ \Delta t \sum_{m=1}^n \|\nabla(\mathbf{u}^m - \frac{\mathbf{u}^{m+1} + \mathbf{u}^{m-1}}{2})\|_0^2 &\leq \frac{7\Delta t^4}{6} \|\mathbf{u}_{tt}\|_{L^2(0,T;H^1(\Omega))}^2 \\ \Delta t \sum_{m=1}^n \|\nabla(\theta^m - \frac{\theta^{m+1} + \theta^{m-1}}{2})\|_0^2 &\leq \frac{7\Delta t^4}{6} \|\theta_{tt}\|_{L^2(0,T;H^1(\Omega))}^2\end{aligned}$$

Proof. The proof of these inequalities is similar to Lemma 3.2 in [16]. \square

Theorem 5.1(Convergence). Assume that the true solution (\mathbf{u}, p, θ) satisfies the regularity conditions $\mathbf{u} \in L^2(0, T, H^4(\Omega)^2) \cap L^\infty(0, T, H^3(\Omega)^2) \cap H^3(0, T, H^1(\Omega)^2)$, $p \in L^2(0, T, L^2(\Omega))$, $\theta \in L^2(0, T, H^4(\Omega)) \cap L^\infty(0, T, H^3(\Omega)) \cap H^3(0, T, H^1(\Omega))$ and the initial approximations are accurate. For $m = 1, 2, \dots, n, n := M - 1$

$$\begin{aligned}&(\|\mathbf{e}^{n+1}\|_0^2 + \|\mathbf{e}^n\|_0^2) + (\|\epsilon^{n+1}\|_0^2 + \|\epsilon^n\|_0^2) \\ &+ \frac{\nu \Delta t}{4} \sum_{m=1}^n \|\mathbf{e}^{m+1} + \mathbf{e}^{m-1}\|_1^2 + \frac{5\lambda\nu\Delta t}{8} \sum_{m=1}^n \|(\epsilon^{m+1} + \epsilon^{m-1})\|_1^2 \\ &\leq \hat{C}(\Delta t^4 + h^{2s_1} + h^{2m_1} + h^{2(m_1+1)})\end{aligned}\tag{5.1}$$

$$\text{where } \hat{C} = \exp(\Delta t \sum_{m=1}^n \max\{\frac{96C^2}{\lambda\nu}, \frac{96C^2}{\nu}, 64k^2\nu^3\mathbf{g}^2C_P^2\})$$

Proof. First, we take the form of (2.2) at time $t = t^m$ and combine the Lemma 3.1, for $\forall \mathbf{v}_h \in V_h, q_h \in Q_h, \psi_h \in W_h$

$$\begin{aligned}(\mathbf{u}_t^m, \mathbf{v}_h) + a(\mathbf{u}^m, \mathbf{v}_h) + \tilde{b}(\mathbf{v}_h, p^m) - \tilde{b}(\mathbf{u}^m, q_h) + N(\mathbf{u}^m; \mathbf{u}^m, \mathbf{v}_h) &= (-k\nu^2 \mathbf{g} \theta^m, \mathbf{v}_h) + (\mathbf{f}^m, \mathbf{v}_h) \\ (\theta_t^m, \psi_h) + c(\tilde{\theta}^m, \psi_h) + \bar{N}(\mathbf{u}^m; \theta^m, \psi_h) &= (b^m, \psi_h)\end{aligned}\tag{5.2}$$

As V_h is discretely divergence free space, the pressure term $(p_h^m, \nabla \cdot \mathbf{v}_h) = 0$ and $(p^m, \nabla \cdot \mathbf{v}_h) = (p^m - \lambda_h, \nabla \cdot \mathbf{v}_h)$, for any $\lambda_h \in Q_h$. Subtracting (3.4-3.5) from (5.2) and taking $\mathbf{v}_h = \mathbf{e}^{m+1} +$

$e^{m-1}, q_h = 0, \psi_h = \epsilon^{m+1} + \epsilon^{m-1}$, we get:

$$\begin{aligned}
& \left(\frac{\epsilon^{m+1}-e^{m-1}}{2\Delta t}, e^{m+1} + e^{m-1} \right) + \left(\frac{\epsilon^{m+1}-\epsilon^{m-1}}{2\Delta t}, e^{m+1} + e^{m-1} \right) \\
& + a\left(\frac{e^{m+1}+e^{m-1}}{2}, e^{m+1} + e^{m-1}\right) + c\left(\frac{\epsilon^{m+1}+\epsilon^{m-1}}{2}, e^{m+1} + e^{m-1}\right) \\
& \leq \left(\frac{\tilde{u}^{m+1}-\tilde{u}^{m-1}}{2\Delta t} - u_t^m, e^{m+1} + e^{m-1} \right) + \left(\frac{\tilde{\theta}^{m+1}-\tilde{\theta}^{m-1}}{2\Delta t} - \theta_t^m, e^{m+1} + e^{m-1} \right) \\
& + a\left(\frac{\tilde{u}^{m+1}+\tilde{u}^{m-1}}{2} - u^m, e^{m+1} + e^{m-1}\right) + c\left(\frac{\tilde{\theta}^{m+1}+\tilde{\theta}^{m-1}}{2} - \tilde{\theta}^m, e^{m+1} + e^{m-1}\right) \\
& + |N(u^m; u^m, e^{m+1} + e^{m-1}) - N(u_h^m; \frac{u_h^{m+1}+u_h^{m-1}}{2}, e^{m+1} + e^{m-1})| \\
& + |\bar{N}(u^m; \theta^m, \epsilon^{m+1} + \epsilon^{m-1}) - \bar{N}(u_h^m; \frac{\theta_h^{m+1}+\theta_h^{m-1}}{2}, \epsilon^{m+1} + \epsilon^{m-1})| \\
& - (k\nu^2 g\epsilon_1^m, e^{m+1} + e^{m-1}) - (k\nu^2 g\epsilon^m, e^{m+1} + e^{m-1}) \\
& + (p^m - \lambda_h, \nabla \cdot (e^{m+1} + e^{m-1})) \\
& = \sum_{i=1}^6 B_i
\end{aligned} \tag{5.3}$$

For any $\varepsilon_1 > 0$, the B_1 can be bounded by using Hölder, Poincaré and Young inequalities:

$$\begin{aligned}
|B_1| &= |(\frac{u^{m+1}-u^{m-1}}{2\Delta t} - u_t^m, e^{m+1} + e^{m-1}) - (\frac{e_1^{m+1}-e_1^{m-1}}{2\Delta t}, e^{m+1} + e^{m-1}) \\
&\quad + (\frac{\theta^{m+1}-\theta^{m-1}}{2\Delta t} - \theta_t^m, e^{m+1} + e^{m-1}) - (\frac{\epsilon_1^{m+1}-\epsilon_1^{m-1}}{2\Delta t}, e^{m+1} + e^{m-1})| \\
&\leq 2\nu\varepsilon_1 \|e^{m+1} + e^{m-1}\|_1^2 + \frac{C_P^2}{\nu\varepsilon_1} \|\frac{u^{m+1}-u^{m-1}}{2\Delta t} - u_t^m\|_0^2 \\
&\quad + 2\lambda\nu\varepsilon_1 \|(\epsilon^{m+1} + \epsilon^{m-1})\|_1^2 + \frac{\tilde{C}_P^2}{\varepsilon_1\lambda\nu} \|\frac{\theta^{m+1}-\theta^{m-1}}{2\Delta t} - \theta_t^m\|_0^2 \\
&\quad + \frac{C_P^2}{\nu\varepsilon_1\Delta t^2} \int_{\Omega} 2\Delta t \int_{t^{m-1}}^{t^{m+1}} |e_{1t}|^2 dt dx + \frac{\tilde{C}_P^2}{\varepsilon_1\lambda\nu\Delta t^2} \int_{\Omega} 2\Delta t \int_{t^{m-1}}^{t^{m+1}} |\epsilon_{1t}|^2 dt dx.
\end{aligned} \tag{5.4}$$

For any $\varepsilon_2 > 0$, the B_2 can be estimated by the continuity of $a(\cdot, \cdot), c(\cdot, \cdot)$, Young inequalities:

$$\begin{aligned}
|B_2| &\leq \nu \|\nabla(\frac{\tilde{u}^{m+1}+\tilde{u}^{m-1}}{2} - \tilde{u}^m)\|_0 \|\nabla(e^{m+1} + e^{m-1})\|_0 + \nu \|\nabla e_1^m\|_0 \|\nabla(e^{m+1} + e^{m-1})\|_0 \\
&\quad + \lambda\nu \|\nabla(\frac{\tilde{\theta}^{m+1}+\tilde{\theta}^{m-1}}{2} - \tilde{\theta}^m)\|_0 \|\nabla(\epsilon^{m+1} + \epsilon^{m-1})\|_0 \\
&\leq \frac{C^2\nu}{\varepsilon_2} \|\nabla(\frac{u^{m+1}+u^{m-1}}{2} - u^m)\|_0^2 + \frac{\nu}{\varepsilon_2} \|\nabla e_1^m\|_0^2 + 2\nu\varepsilon_2 \|\nabla(e^{m+1} + e^{m-1})\|_0^2 \\
&\quad + \frac{C^2\lambda\nu}{\varepsilon_2} \|\nabla(\frac{\theta^{m+1}+\theta^{m-1}}{2} - \theta^m)\|_0^2 + \lambda\nu\varepsilon_2 \|\nabla(\epsilon^{m+1} + \epsilon^{m-1})\|_0^2,
\end{aligned} \tag{5.5}$$

For any $\varepsilon_3 > 0$, the B_3 can be bounded by (2.1) and Hölder, Young inequalities:

$$\begin{aligned}
|B_3| &= |N(u^m; u^m, e^{m+1} + e^{m-1}) - N(u_h^m; \frac{u_h^{m+1}+u_h^{m-1}}{2}, e^{m+1} + e^{m-1})| \\
&= N(u^m - \frac{u^{m+1}+u^{m-1}}{2}; u^m, e^{m+1} + e^{m-1}) + N(\frac{e_1^{m+1}+e_1^{m-1}}{2}; u^m, e^{m+1} + e^{m-1}) \\
&\quad + N(\frac{\tilde{u}^{m+1}+\tilde{u}^{m-1}}{2}; e_1^m, e^{m+1} + e^{m-1}) + N(\frac{\tilde{u}^{m+1}+\tilde{u}^{m-1}}{2}; \tilde{u}^m - \frac{\tilde{u}^{m+1}+\tilde{u}^{m-1}}{2}, e^{m+1} + e^{m-1}) \\
&\quad + N(\frac{\tilde{u}^{m+1}+\tilde{u}^{m-1}}{2} - \tilde{u}^m; \frac{\tilde{u}^{m+1}+\tilde{u}^{m-1}}{2}, e^{m+1} + e^{m-1}) + N(e^m; \frac{u^{m+1}+u^{m-1}}{2}, e^{m+1} + e^{m-1}) \\
&\quad - N(e^m; \frac{e_1^{m+1}+e_1^{m-1}}{2}, e^{m+1} + e^{m-1}) + N(u_h^m; \frac{e^{m+1}+e^{m-1}}{2}, e^{m+1} + e^{m-1}) \\
&\leq 7\nu\varepsilon_3 \|e^{m+1} + e^{m-1}\|_1^2 + \frac{C^2}{\nu\varepsilon_3} \|\nabla(u^m - \frac{u^{m+1}+u^{m-1}}{2})\|_0^2 + \frac{C^2}{\nu\varepsilon_3} \|\frac{e_1^{m+1}+e_1^{m-1}}{2}\|_0^2 \\
&\quad + \frac{C^2}{\nu\varepsilon_3} \|e_1^m\|_1^2 + \frac{2C^2}{\nu\varepsilon_3} \|\nabla(u^m - \frac{u^{m+1}+u^{m-1}}{2})\|_0^2 + \frac{C^2}{\nu\varepsilon_3} \|e^m\|_0^2.
\end{aligned} \tag{5.6}$$

For any $\varepsilon_4 > 0$, the B_4 can be bounded by a similar technique:

$$\begin{aligned}
|B_4| &= |\bar{N}(\mathbf{u}^m; \theta^m, \epsilon^{m+1} + \epsilon^{m-1}) - \bar{N}(\mathbf{u}_h^m; \frac{\theta_h^{m+1} + \theta_h^{m-1}}{2}, \epsilon^{m+1} + \epsilon^{m-1})| \\
&= \bar{N}(\mathbf{u}^m - \frac{\mathbf{u}^{m+1} + \mathbf{u}^{m-1}}{2}; \theta^m, \epsilon^{m+1} + \epsilon^{m-1}) + \bar{N}(\frac{\mathbf{e}_1^{m+1} + \mathbf{e}_1^{m-1}}{2}; \theta^m, \epsilon^{m+1} + \epsilon^{m-1}) \\
&\quad + \bar{N}(\frac{\tilde{\mathbf{u}}^{m+1} + \tilde{\mathbf{u}}^{m-1}}{2}; \epsilon_1^m, \epsilon^{m+1} + \epsilon^{m-1}) + \bar{N}(\frac{\tilde{\mathbf{u}}^{m+1} + \tilde{\mathbf{u}}^{m-1}}{2}; \tilde{\theta}^m - \frac{\tilde{\theta}^{m+1} + \tilde{\theta}^{m-1}}{2}, \epsilon^{m+1} + \epsilon^{m-1}) \\
&\quad + \bar{N}(\frac{\tilde{\mathbf{u}}^{m+1} + \tilde{\mathbf{u}}^{m-1}}{2} - \tilde{\mathbf{u}}^m; \frac{\tilde{\theta}^{m+1} + \tilde{\theta}^{m-1}}{2}, \epsilon^{m+1} + \epsilon^{m-1}) + \bar{N}(\mathbf{e}^m; \frac{\theta^{m+1} + \theta^{m-1}}{2}, \epsilon^{m+1} + \epsilon^{m-1}) \\
&\quad - \bar{N}(\mathbf{e}^m; \frac{\epsilon_1^{m+1} + \epsilon_1^{m-1}}{2}, \epsilon^{m+1} + \epsilon^{m-1}) + \bar{N}(\mathbf{u}_h^m; \frac{\epsilon^{m+1} + \epsilon^{m-1}}{2}, \epsilon^{m+1} + \epsilon^{m-1}) \\
&\leq 7\lambda\nu\varepsilon_4 \|\epsilon^{m+1} + \epsilon^{m-1}\|_1^2 + \frac{C^2}{\lambda\nu\varepsilon_4} \|\nabla(\mathbf{u}^m - \frac{\mathbf{u}^{m+1} + \mathbf{u}^{m-1}}{2})\|_0^2 + \frac{C^2}{\lambda\nu\varepsilon_4} \|\frac{\mathbf{e}_1^{m+1} + \mathbf{e}_1^{m-1}}{2}\|_0^2 \\
&\quad + \frac{C^2}{\lambda\nu\varepsilon_4} \|\epsilon_1^m\|_1^2 + \frac{C^2}{\lambda\nu\varepsilon_4} \|\nabla(\theta^m - \frac{\theta^{m+1} + \theta^{m-1}}{2})\|_0^2 + \frac{C^2}{\lambda\nu\varepsilon_4} \|\nabla(\mathbf{u}^m - \frac{\mathbf{u}^{m+1} + \mathbf{u}^{m-1}}{2})\|_0^2 + \frac{C^2}{\lambda\nu\varepsilon_4} \|\mathbf{e}^m\|_0^2.
\end{aligned} \tag{5.7}$$

For any $\varepsilon_5 > 0$, the B_5 can be bounded by Hölder and Young inequalities :

$$\begin{aligned}
|B_5| &= |-(k\nu^2 \mathbf{g} \epsilon_1^m, \mathbf{e}^{m+1} + \mathbf{e}^{m-1}) - (k\nu^2 \mathbf{g} \epsilon^m, \mathbf{e}^{m+1} + \mathbf{e}^{m-1})| \\
&\leq k\nu^2 \mathbf{g} C_P \|\epsilon_1^m\|_0 \|\mathbf{e}^{m+1} + \mathbf{e}^{m-1}\|_1 + k\nu^2 \mathbf{g} C_P \|\epsilon^m\|_0 \|\mathbf{e}^{m+1} + \mathbf{e}^{m-1}\|_1 \\
&\leq \frac{k^2 \nu^3 \mathbf{g}^2 C_P^2}{\varepsilon_5} \|\epsilon_1^m\|_0^2 + \frac{k^2 \nu^3 \mathbf{g}^2 C_P^2}{\varepsilon_5} \|\epsilon^m\|_0^2 + 2\varepsilon_5 \nu \|\mathbf{e}^{m+1} + \mathbf{e}^{m-1}\|_1^2
\end{aligned} \tag{5.8}$$

For any $\varepsilon_6 > 0$, the B_6 can be bounded by similar approach:

$$|B_6| \leq \frac{d}{\nu\varepsilon_6} \|\eta_1^m\|_0^2 + \nu\varepsilon_6 \|\nabla(\mathbf{e}^{m+1} + \mathbf{e}^{m-1})\|_0^2. \tag{5.9}$$

Substituting (5.4-5.9) into (5.3), multiplying the resulting inequality by $2\Delta t$ and summing from $m = 1$ to $m = n$, choosing $\varepsilon_1 = \frac{1}{64}, \varepsilon_2 = \varepsilon_5 = \frac{1}{32}, \varepsilon_3 = \varepsilon_4 = \frac{1}{48}, \varepsilon_6 = \frac{3}{32}$, we obtain the result:

$$\begin{aligned}
&(\|\mathbf{e}^{n+1}\|_0^2 + \|\mathbf{e}^n\|_0^2) + (\|\epsilon^{n+1}\|_0^2 + \|\epsilon^n\|_0^2) \\
&\quad + \frac{\nu\Delta t}{4} \sum_{m=1}^n \|\mathbf{e}^{m+1} + \mathbf{e}^{m-1}\|_1^2 + \frac{5\lambda\nu\Delta t}{8} \sum_{m=1}^n \|(\epsilon^{m+1} + \epsilon^{m-1})\|_1^2 \\
&\leq \frac{128C_P^2\Delta t}{\nu} \sum_{m=1}^n \|\mathbf{u}_t^m - \frac{\mathbf{u}^{m+1} - \mathbf{u}^{m-1}}{2\Delta t}\|_0^2 + \frac{128\tilde{C}_P^2\Delta t}{\lambda\nu} \sum_{m=1}^n \|\theta_t^m - \frac{\theta^{m+1} - \theta^{m-1}}{2\Delta t}\|_0^2 \\
&\quad + \frac{512C_P^2}{\nu} \|\mathbf{e}_{1t}\|_{L^2(0,T;L^2(\Omega))}^2 + \frac{512gS_0^2\tilde{C}_P^2}{\lambda\nu} \|\epsilon_{1t}\|_{L^2(0,T;L^2(\Omega))}^2 + 64\nu\Delta t \sum_{m=1}^n \|\nabla \mathbf{e}_1^m\|_0^2 \\
&\quad + \frac{64C^2\Delta t}{\nu} \sum_{m=1}^n \|\nabla(\mathbf{u}^m - \frac{\mathbf{u}^{m+1} + \mathbf{u}^{m-1}}{2})\|_0^2 + \frac{64C^2\Delta t}{\lambda\nu} \sum_{m=1}^n \|\nabla(\theta^m - \frac{\theta^{m+1} + \theta^{m-1}}{2})\|_0^2 \\
&\quad + \frac{96C^2\Delta t}{\nu} \sum_{m=1}^n \|\nabla(\mathbf{u}^m - \frac{\mathbf{u}^{m+1} + \mathbf{u}^{m-1}}{2})\|_0^2 + \frac{96C^2\Delta t}{\nu} \sum_{m=1}^n \|\frac{\mathbf{e}_1^{m+1} + \mathbf{e}_1^{m-1}}{2}\|_0^2 \\
&\quad + \frac{96C^2\Delta t}{\nu} \sum_{m=1}^k \|\mathbf{e}_1^m\|_1^2 + \frac{192C^2\Delta t}{\nu} \sum_{m=1}^n \|\nabla(\mathbf{u}^m - \frac{\mathbf{u}^{m+1} + \mathbf{u}^{m-1}}{2})\|_0^2
\end{aligned}$$

$$\begin{aligned}
& + \frac{96C^2\Delta t}{\lambda\nu} \sum_{m=1}^n \|\nabla(\mathbf{u}^m - \frac{\mathbf{u}^{m+1}+\mathbf{u}^{m-1}}{2})\|_0^2 + \frac{96C^2\Delta t}{\lambda\nu} \sum_{m=1}^n \|\frac{\mathbf{e}_1^{m+1}+\mathbf{e}_1^{m-1}}{2}\|_0^2 \\
& + \frac{96C^2\Delta t}{\lambda\nu} \sum_{m=1}^k \|\mathbf{e}_1^m\|_1^2 + \frac{96C^2\Delta t}{\lambda\nu} \sum_{m=1}^n \|\nabla(\mathbf{u}^m - \frac{\mathbf{u}^{m+1}+\mathbf{u}^{m-1}}{2})\|_0^2 \\
& + \frac{96C^2\Delta t}{\lambda\nu} \sum_{m=1}^n \|\nabla(\theta^m - \frac{\theta^{m+1}+\theta^{m-1}}{2})\|_0^2 + \frac{96C^2\Delta t}{\lambda\nu} \sum_{m=1}^n \|\mathbf{e}^m\|_0^2 + \frac{96C^2\Delta t}{\nu} \sum_{m=1}^n \|\mathbf{e}^m\|_0^2 \\
& + 64k^2\nu^3\mathbf{g}^2C_P^2\Delta t \sum_{m=1}^n \|\epsilon_1^m\|_0^2 + \frac{64d\Delta t}{3\nu} \sum_{m=1}^n \|\eta_1^m\|_0^2 + 64k^2\nu^3\mathbf{g}^2C_P^2\Delta t \sum_{m=1}^n \|\epsilon^m\|_0^2. \tag{5.10}
\end{aligned}$$

By using Lemma 5.1, (3.1) and (3.3), we get

$$\begin{aligned}
& (\|\mathbf{e}^{n+1}\|_0^2 + \|\mathbf{e}^n\|_0^2) + (\|\epsilon^{n+1}\|_0^2 + \|\epsilon^n\|_0^2) \\
& + \frac{5\nu\Delta t}{24} \sum_{m=1}^n \|\mathbf{e}^{m+1} + \mathbf{e}^{m-1}\|_1^2 + \frac{7\lambda\nu\Delta t}{12} \sum_{m=1}^n \|(\epsilon^{m+1} + \epsilon^{m-1})\|_1^2 \\
& \leq C(\Delta t^4 + h^{2s_1} + h^{2m_1} + h^{2(m_1+1)}) + (\|\mathbf{e}^1\|_0^2 + \|\mathbf{e}^0\|_0^2) + (\|\epsilon^1\|_0^2 + \|\epsilon^0\|_0^2) \\
& + \frac{96C^2\Delta t}{\lambda\nu} \sum_{m=1}^n \|\mathbf{e}^m\|_0^2 + \frac{96C^2\Delta t}{\nu} \sum_{m=1}^n \|\mathbf{e}^m\|_0^2 + 64k^2\nu^3\mathbf{g}^2C_P^2\Delta t \sum_{m=1}^n \|\epsilon^m\|_0^2. \tag{5.11}
\end{aligned}$$

Using Lemma 4.1, we complete the proof. \square

Corollary 5.1. For $m = 1, 2, \dots, M$, the following estimates hold:

$$\begin{aligned}
\|(\mathbf{u} - \mathbf{u}_h)(t_m)\|_{L^\infty(0,T;L^2(\Omega))} & \leq C(\Delta t^2 + h^{s_1} + h^{m_1} + h^{m_1+1}) \\
\|(\theta - \theta_h)(t_m)\|_{L^\infty(0,T;L^2(\Omega))} & \leq C(\Delta t^2 + h^{s_1} + h^{m_1} + h^{m_1+1}).
\end{aligned}$$

Proof. By Theorem 5.1 and (3.1), using the triangle inequality, the result can be obtained. \square

6 The Numerical Experiments

6.1 Convergence rate

In the section, numerical examples are provided to verify the theoretical analysis in the previous sections. The software Freefem++ developed by Hecht et al.[22] is used in our experiments. The domain Ω is subdivided by triangular elements in Fig 1. We will use $P_2 - P_1 - P_2$ elements or $P_{1b} - P_1 - P_1$ elements to approximate the velocity \mathbf{u} , the pressure p and the temperature θ , respectively. To explain the accuracy of our numerical schemes, first of all, we assume that the error estimate is $O(\Delta t^{\alpha_1} + h^{\alpha_2})$. Let $\Delta t = h^\alpha$, we quantify the convergence rate that was defined in [23] $rate = \min\{\alpha\alpha_1, \alpha_2\}$ with respect to h by calculating $rate = \log(ER/\hat{ER})/\log(h/\hat{h})$, where h, \hat{h} represent two consecutive mesh sizes and ER, \hat{ER} are corresponding error norms.

Let the domain $\Omega = [0, 1] \times [0, 1]$, the parameters $\nu = \lambda = k = 1.0, T = 1.0$ and true solutions in [7] \mathbf{u}, p, θ are:

$$\begin{aligned}
\mathbf{u} &= (u1, u2) = (10x^2(x-1)^2y(y-1)(2y-1)\cos(t), -10y^2(y-1)^2x(x-1)(2x-1)\cos(t)), \\
p &= 10(2x-1)(2y-1)\cos(t), \\
\theta &= 10x^2(x-1)^2y(y-1)(2y-1)\cos(t) - 10y^2(y-1)^2x(x-1)(2x-1)\cos(t).
\end{aligned}$$

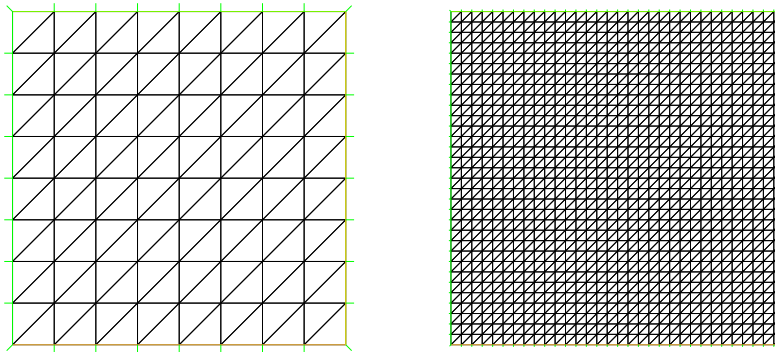


Fig 1: Domain Ω with 8 nodes(left) and 32 nodes (right) per domain side.

The initial conditions, boundary conditions, and forcing terms can be obtained by substituting the true solutions into model equations.

In Tables 1-2, we presented the error estimates and convergence rates obtained by the decoupled CNLF method ($P_2 - P_1 - P_2, P_{1b} - P_1 - P_1$) at time $T = 1$ achieved with varying time step and mesh sizes $\Delta t = h = \frac{1}{4}, \frac{1}{8}, \frac{1}{16}, \frac{1}{32}, \frac{1}{64}$. Numerical results show the order of convergence of the decoupled CNLF methods ($P_{1b} - P_1 - P_1$) is $O(\Delta t^2 + h^2)$ for both \mathbf{u}_h and θ_h in the L^2 -norm, and the order of convergence of the decoupled CNLF methods ($P_2 - P_1 - P_2$) are $O(\Delta t^2)$ for both \mathbf{u}_h and θ_h in the L^2 -norm.

In Tables 3, we assume that $\Delta t = \frac{1}{10}h, h = \frac{1}{2}, \frac{1}{4}, \frac{1}{8}, \frac{1}{16}, \frac{1}{32}$. Numerical results show the orders of convergence of the decoupled CNLF methods ($P_2 - P_1 - P_2$) are $O(h^3)$ for both \mathbf{u}_h and θ_h in the L^2 -norm.

To illustrate the effectiveness of the CNLF scheme, we compute the error norms and convergence order that are obtained by the Crank-Nicolson linear extrapolation(CNLE) and Crank-Nicolson linear extrapolation stabilized(CNSLE) methods in [8]. In Tables 2-7, under the same true solutions and physical parameters, we can obtain the fact that compared to the CNLE and CNSLE methods, when the same accuracy and convergence order are maintained, the decoupled CNLF method can save a lot of CPU time.

Remark. The CNLE method can be obtained when the stabilized parameter μ in the CNSLE method is equal to 0.

Table 1: Errors and rates for the decoupled CNLF method using the $P_2 - P_1 - P_2$ with $T = 1.0$.

| $\Delta t = h$ | $\frac{\ \mathbf{u} - \mathbf{u}_h\ _0}{\ \mathbf{u}\ _0}$ | rate | $\frac{\ \mathbf{u} - \mathbf{u}_h\ _1}{\ \mathbf{u}\ _1}$ | rate | $\frac{\ p - p_h\ _0}{\ p\ _0}$ | rate |
|----------------|--|---------|--|---------|---------------------------------|---------|
| $\frac{1}{4}$ | 0.0831559 | | 0.279123 | | 0.0494035 | |
| $\frac{1}{8}$ | 0.0107836 | 2.94698 | 0.0662541 | 2.07482 | 0.0113641 | 2.12013 |
| $\frac{1}{16}$ | 0.00222631 | 2.27611 | 0.0143395 | 2.20802 | 0.00261308 | 2.12066 |
| $\frac{1}{32}$ | 0.000510129 | 2.12572 | 0.00352718 | 2.02341 | 0.000660926 | 1.98319 |
| $\frac{1}{64}$ | 0.000124479 | 2.03497 | 0.000934829 | 1.91574 | 0.00016749 | 1.98042 |
| $\Delta t = h$ | $\frac{\ \theta - \theta_h\ _0}{\ \theta\ _0}$ | rate | $\frac{\ \theta - \theta_h\ _1}{\ \theta\ _1}$ | rate | CPU(s) | |
| $\frac{1}{4}$ | 0.0442024 | | 0.180356 | | 0.087 | |
| $\frac{1}{8}$ | 0.00590384 | 2.9044 | 0.0390744 | 2.20656 | 0.664 | |
| $\frac{1}{16}$ | 0.00199917 | 1.56226 | 0.00858695 | 2.186 | 5.687 | |
| $\frac{1}{32}$ | 0.000500187 | 1.99886 | 0.00214667 | 2.00005 | 60.423 | |
| $\frac{1}{64}$ | 0.000124694 | 2.00408 | 0.000560782 | 1.93659 | 1042.31 | |

Table 2: Errors and rates for the decoupled CNLF method using the $P_{1b} - P_1 - P_1$ with $T = 1.0$.

| $\Delta t = h$ | $\frac{\ \mathbf{u} - \mathbf{u}_h\ _0}{\ \mathbf{u}\ _0}$ | rate | $\frac{\ \mathbf{u} - \mathbf{u}_h\ _1}{\ \mathbf{u}\ _1}$ | rate | $\frac{\ p - p_h\ _0}{\ p\ _0}$ | rate |
|----------------|--|---------|--|----------|---------------------------------|---------|
| $\frac{1}{4}$ | 0.216675 | | 1.28646 | | 0.062091 | |
| $\frac{1}{8}$ | 0.0670149 | 1.69298 | 0.688718 | 0.901424 | 0.0203799 | 1.60724 |
| $\frac{1}{16}$ | 0.0179769 | 1.89834 | 0.305051 | 1.17486 | 0.00531066 | 1.94018 |
| $\frac{1}{32}$ | 0.00472645 | 1.92732 | 0.155 | 0.976784 | 0.00220386 | 1.26886 |
| $\frac{1}{64}$ | 0.001237 | 1.93391 | 0.0797615 | 0.958504 | 0.000969352 | 1.18494 |
| $\Delta t = h$ | $\frac{\ \theta - \theta_h\ _0}{\ \theta\ _0}$ | rate | $\frac{\ \theta - \theta_h\ _1}{\ \theta\ _1}$ | rate | CPU(s) | |
| $\frac{1}{4}$ | 0.319484 | | 0.614972 | | 0.083 | |
| $\frac{1}{8}$ | 0.0857203 | 1.89803 | 0.326337 | 0.914156 | 0.542 | |
| $\frac{1}{16}$ | 0.0186624 | 2.1995 | 0.146129 | 1.15912 | 4.553 | |
| $\frac{1}{32}$ | 0.00471327 | 1.98533 | 0.0739761 | 0.982111 | 44.023 | |
| $\frac{1}{64}$ | 0.00126476 | 1.89787 | 0.0380393 | 0.959567 | 623.403 | |

6.2 Temperature-driven cavity flow

This section gives a classic example whose exact solution is not yet known to test the reliability of the numerical method. Consider the thermally driven cavity flow in a closed domain $\Omega = [0, 1] \times [0, 1]$, as shown in Fig 2.

First of all, the example [24-26] on the left side of the Fig 2 is considered. The decoupled CNLF scheme is used. Considering the CNLF format is a three-level method, the value of \mathbf{u}^1, θ^1 needs to be calculated by using Crank-Nicolson linear extrapolation scheme. The physical parameters involved are selected as: $k = 10^5, \nu = 1.0, \lambda = 1.0, \Delta t = 0.0001, h = \frac{1}{32}$. Fig 3 not only gives the streamlines (First column) and isotherms (Third column) at $t = 0.003, 0.01, 0.025, 0.1, 0.2$, but also presents pressure contours(Second column) at $t =$

Table 3: Errors and rates for the decoupled CNLF method using the $P_2 - P_1 - P_2$ with $\Delta t = \frac{1}{10}h$.

| h | $\frac{\ \mathbf{u} - \mathbf{u}_h\ _0}{\ \mathbf{u}\ _0}$ | $rate$ | $\frac{\ \mathbf{u} - \mathbf{u}_h\ _1}{\ \mathbf{u}\ _1}$ | $rate$ | $\frac{\ p - p_h\ _0}{\ p\ _0}$ | $rate$ |
|----------------|--|---------|--|---------|---------------------------------|---------|
| $\frac{1}{2}$ | 1.34595 | | 1.98379 | | 0.318492 | |
| $\frac{1}{4}$ | 0.0863908 | 3.9616 | 0.279702 | 2.8263 | 0.0493627 | 2.68976 |
| $\frac{1}{8}$ | 0.0124917 | 2.78991 | 0.0692151 | 2.01473 | 0.0113618 | 2.11923 |
| $\frac{1}{16}$ | 0.0014081 | 3.14915 | 0.0153843 | 2.16963 | 0.00261289 | 2.12047 |
| $\frac{1}{32}$ | 0.000171455 | 3.03784 | 0.00375608 | 2.03416 | 0.00066091 | 1.98312 |
| h | $\frac{\ \theta - \theta_h\ _0}{\ \theta\ _0}$ | $rate$ | $\frac{\ \theta - \theta_h\ _1}{\ \theta\ _1}$ | $rate$ | CPU(s) | |
| $\frac{1}{2}$ | 0.30538 | | 0.597688 | | 0.231 | |
| $\frac{1}{4}$ | 0.0444182 | 2.78138 | 0.166724 | 1.84193 | 1.141 | |
| $\frac{1}{8}$ | 0.00444218 | 3.32181 | 0.0364687 | 2.19273 | 7.453 | |
| $\frac{1}{16}$ | 0.000463517 | 3.26057 | 0.00795744 | 2.19628 | 60.058 | |
| $\frac{1}{32}$ | 5.73182e-05 | 3.01556 | 0.00198086 | 2.00618 | 621.203 | |

Table 4: Errors and rates for the CNLE method using the $P_2 - P_1 - P_2$ with $\Delta t = \frac{1}{10}h$.

| h | $\frac{\ \mathbf{u} - \mathbf{u}_h\ _0}{\ \mathbf{u}\ _0}$ | $rate$ | $\frac{\ \mathbf{u} - \mathbf{u}_h\ _1}{\ \mathbf{u}\ _1}$ | $rate$ | $\frac{\ p - p_h\ _0}{\ p\ _0}$ | $rate$ |
|----------------|--|---------|--|---------|---------------------------------|---------|
| $\frac{1}{2}$ | 1.43173 | | 2.10379 | | 0.511749 | |
| $\frac{1}{4}$ | 0.0910992 | 3.97418 | 0.303873 | 2.79145 | 0.061536 | 3.05593 |
| $\frac{1}{8}$ | 0.0129113 | 2.8188 | 0.0762458 | 1.99474 | 0.0148998 | 2.04613 |
| $\frac{1}{16}$ | 0.0014526 | 3.15193 | 0.0166811 | 2.19244 | 0.00311537 | 2.25782 |
| $\frac{1}{32}$ | 0.000177706 | 3.03107 | 0.00409406 | 2.02661 | 0.000836275 | 1.89735 |
| h | $\frac{\ \theta - \theta_h\ _0}{\ \theta\ _0}$ | $rate$ | $\frac{\ \theta - \theta_h\ _1}{\ \theta\ _1}$ | $rate$ | CPU(s) | |
| $\frac{1}{2}$ | 0.308949 | | 0.595619 | | 0.513 | |
| $\frac{1}{4}$ | 0.0449427 | 2.78121 | 0.164877 | 1.853 | 2.21 | |
| $\frac{1}{8}$ | 0.0044856 | 3.32471 | 0.0362809 | 2.18411 | 14.553 | |
| $\frac{1}{16}$ | 0.000465435 | 3.26865 | 0.00791897 | 2.19582 | 122.831 | |
| $\frac{1}{32}$ | 5.74498e-05 | 3.01821 | 0.00197239 | 2.00537 | 1395.22 | |

0.0029, 0.0099, 0.0249, 0.0999, 0.1999.

Then, the example [5,7] on the right side of the Fig 2 is considered. The physical parameters involved are set: $\nu = 0.71$, $\lambda = 1.0$, $\Delta t = 0.01$, $h = \frac{1}{50}$, and $k = 1400, 14000, t = 10$. Fig 4 gives the streamlines (First line) and isotherms (Second line) at different Groshoff number.

By observing Fig 3-4, these results are in agreement with the published works, which shows the effectiveness of the decoupled CNLF algorithm for practical problems.

Table 5: Errors and rates for the CNLE method using the $P_{1b} - P_1 - P_1$ with $T = 1.0$.

| $\Delta t = h$ | $\frac{\ \mathbf{u} - \mathbf{u}_h\ _0}{\ \mathbf{u}\ _0}$ | rate | $\frac{\ \mathbf{u} - \mathbf{u}_h\ _1}{\ \mathbf{u}\ _1}$ | rate | $\frac{\ p - p_h\ _0}{\ p\ _0}$ | rate |
|----------------|--|---------|--|----------|---------------------------------|---------|
| $\frac{1}{4}$ | 0.243016 | | 1.23369 | | 0.0763048 | |
| $\frac{1}{8}$ | 0.0853548 | 1.5095 | 0.676834 | 0.866107 | 0.0181789 | 2.06951 |
| $\frac{1}{16}$ | 0.0192773 | 2.14657 | 0.300586 | 1.17102 | 0.00420574 | 2.11183 |
| $\frac{1}{32}$ | 0.00498633 | 1.95085 | 0.152721 | 0.976878 | 0.00131204 | 1.68055 |
| $\frac{1}{64}$ | 0.00128845 | 1.95234 | 0.0785254 | 0.95967 | 0.000499946 | 1.39197 |
| $\Delta t = h$ | $\frac{\ \theta - \theta_h\ _0}{\ \theta\ _0}$ | rate | $\frac{\ \theta - \theta_h\ _1}{\ \theta\ _1}$ | rate | CPU(s) | |
| $\frac{1}{4}$ | 0.327116 | | 0.605237 | | 0.193 | |
| $\frac{1}{8}$ | 0.0904758 | 1.8542 | 0.31899 | 0.92399 | 1.252 | |
| $\frac{1}{16}$ | 0.0200179 | 2.17624 | 0.144805 | 1.1394 | 9.757 | |
| $\frac{1}{32}$ | 0.00505118 | 1.9866 | 0.0730759 | 0.986647 | 89.151 | |
| $\frac{1}{64}$ | 0.00134215 | 1.91208 | 0.0375703 | 0.959802 | 1241.76 | |

Table 6: Errors and rates for the CNSLE method using the $P_2 - P_1 - P_2$ with $\Delta t = \frac{1}{10}h$.

| h | $\frac{\ \mathbf{u} - \mathbf{u}_h\ _0}{\ \mathbf{u}\ _0}$ | rate | $\frac{\ \mathbf{u} - \mathbf{u}_h\ _1}{\ \mathbf{u}\ _1}$ | rate | $\frac{\ p - p_h\ _0}{\ p\ _0}$ | rate |
|----------------|--|---------|--|---------|---------------------------------|---------|
| $\frac{1}{2}$ | 1.42643 | | 2.09625 | | 0.750619 | |
| $\frac{1}{4}$ | 0.110688 | 3.68784 | 0.522036 | 2.00559 | 0.156078 | 2.26582 |
| $\frac{1}{8}$ | 0.0130723 | 3.08192 | 0.0852428 | 2.6145 | 0.0229232 | 2.76738 |
| $\frac{1}{16}$ | 0.0014679 | 3.15469 | 0.0178716 | 2.2539 | 0.0040902 | 2.48657 |
| $\frac{1}{32}$ | 0.000179266 | 3.03357 | 0.00430963 | 2.05204 | 0.00107886 | 1.92266 |
| h | $\frac{\ \theta - \theta_h\ _0}{\ \theta\ _0}$ | rate | $\frac{\ \theta - \theta_h\ _1}{\ \theta\ _1}$ | rate | CPU(s) | |
| $\frac{1}{2}$ | 0.309248 | | 0.596136 | | 0.527 | |
| $\frac{1}{4}$ | 0.0484952 | 2.67285 | 0.221948 | 1.42542 | 2.271 | |
| $\frac{1}{8}$ | 0.00458134 | 3.404 | 0.0394862 | 2.4908 | 14.588 | |
| $\frac{1}{16}$ | 0.000481662 | 3.24968 | 0.00857845 | 2.20256 | 124.755 | |
| $\frac{1}{32}$ | 6.0843e-05 | 2.98486 | 0.0021113 | 2.02259 | 1408.25 | |

Table 7: Errors and rates for the CNSLE method using the $P_{1b} - P_1 - P_1$ with $T = 1.0$.

| $\Delta t = h$ | $\frac{\ \mathbf{u} - \mathbf{u}_h\ _0}{\ \mathbf{u}\ _0}$ | rate | $\frac{\ \mathbf{u} - \mathbf{u}_h\ _1}{\ \mathbf{u}\ _1}$ | rate | $\frac{\ p - p_h\ _0}{\ p\ _0}$ | rate |
|----------------|--|---------|--|----------|---------------------------------|---------|
| $\frac{1}{4}$ | 0.311834 | | 1.78284 | | 0.0757661 | |
| $\frac{1}{8}$ | 0.0983512 | 1.66477 | 0.960749 | 0.891946 | 0.0182378 | 2.05462 |
| $\frac{1}{16}$ | 0.0219843 | 2.16147 | 0.423901 | 1.18043 | 0.00434667 | 2.06895 |
| $\frac{1}{32}$ | 0.00566979 | 1.95511 | 0.215372 | 0.976898 | 0.00134832 | 1.68875 |
| $\frac{1}{64}$ | 0.00146463 | 1.95276 | 0.11088 | 0.957823 | 0.000515811 | 1.38624 |
| $\Delta t = h$ | $\frac{\ \theta - \theta_h\ _0}{\ \theta\ _0}$ | rate | $\frac{\ \theta - \theta_h\ _1}{\ \theta\ _1}$ | rate | CPU(s) | |
| $\frac{1}{4}$ | 0.327697 | | 0.636026 | | 0.178 | |
| $\frac{1}{8}$ | 0.0937558 | 1.80538 | 0.336257 | 0.919523 | 1.179 | |
| $\frac{1}{16}$ | 0.0206814 | 2.18058 | 0.147784 | 1.18607 | 9.157 | |
| $\frac{1}{32}$ | 0.00523878 | 1.98103 | 0.0749969 | 0.978589 | 84.717 | |
| $\frac{1}{64}$ | 0.0013906 | 1.91352 | 0.0385898 | 0.958612 | 1167.97 | |

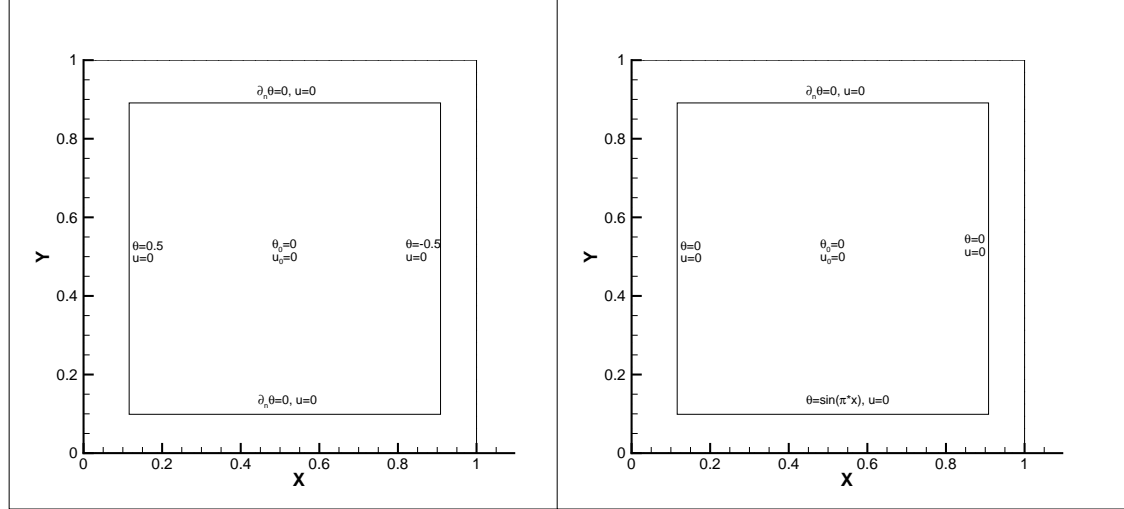


Fig 2 the thermally driven cavity flow: Initial values and boundary conditions.

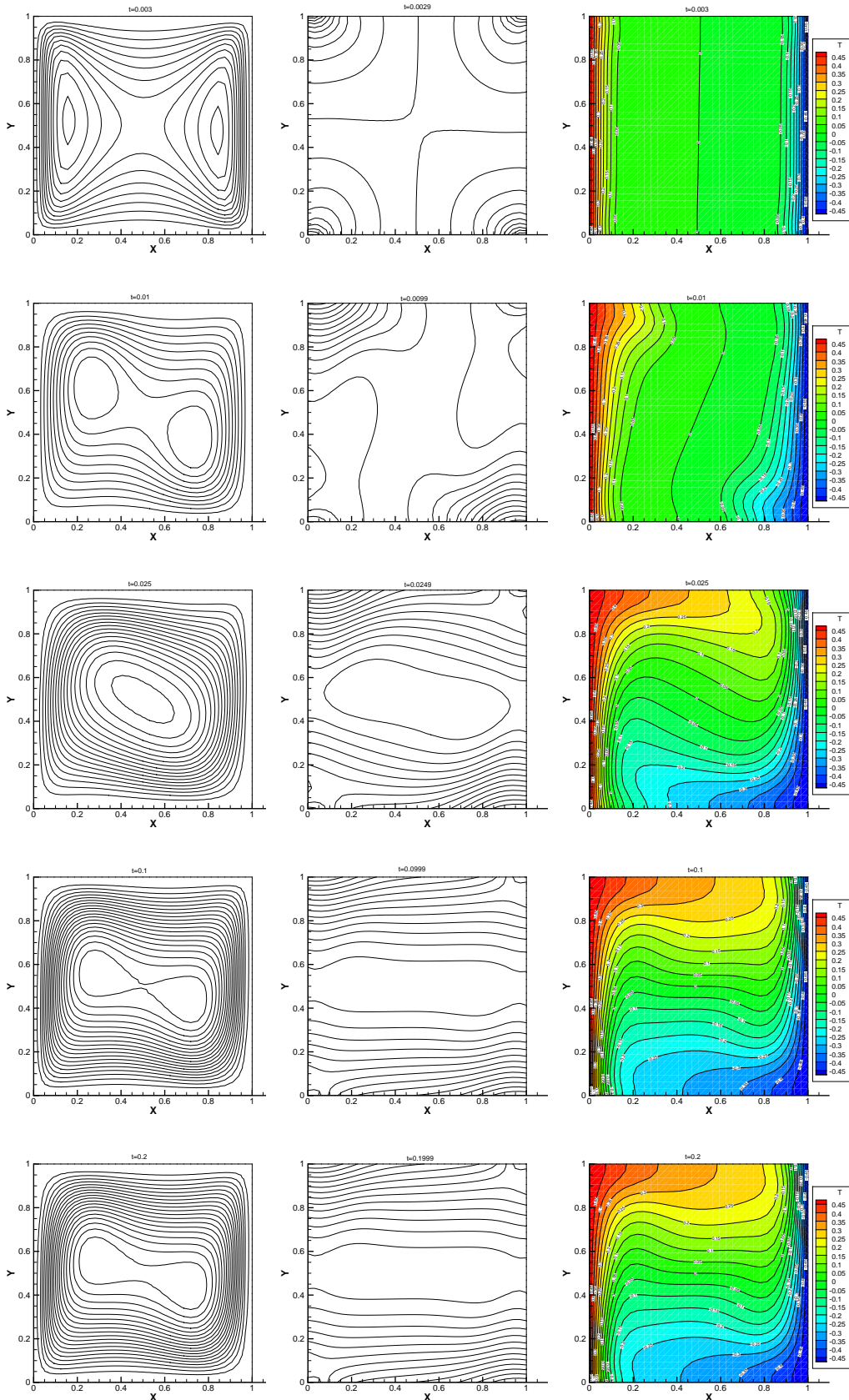


Fig 3 the decoupled CNLF algorithm: first column: streamline, second column: pressure contours, third column: isotherms at different times.

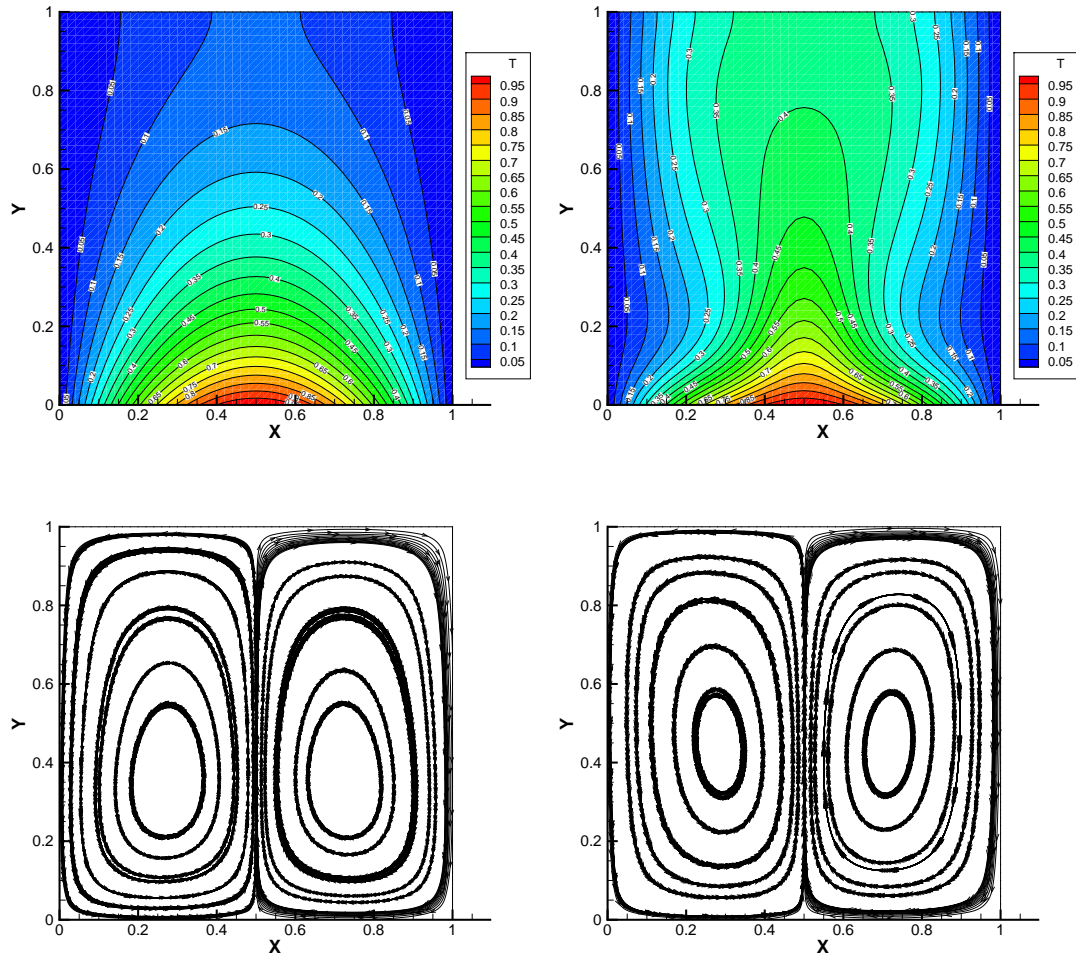


Fig 4 the decoupled CNLF algorithm: first line:streamlines, second line:isotherms at different Groshoff number $k = 1400, 14000$.

7 Conclusion

In this paper, we have provided theoretical analysis of the decoupled CNLF method for solving the evolution Boussinesq equations. Numerical experiments show that the decoupled CNLF method is second order in time and space for the L^2 -norm of \mathbf{u}_h and θ_h . Compared to the CNLE(CNSLE) scheme, when the same accuracy is maintained, numerical results show that the new method can save a lot of CPU time.

References

- [1] J. Pedloski, Geophysical Fluid Dynamics, Springer-Verlag, New York, 1987
- [2] B. Climent-Ezquerro, F. Guillén-González, M.A. Rojas-Medar, Time-periodic solutions for a generalized Boussinesq model with Neumann boundary conditions for temperature, Proc. Roy. Soc. A, 2007;463(2085):2153-2164.
- [3] M. Lewicka, P.B. Mucha, On the existence of traveling waves in the 3D Boussinesq system, Comm. Math. Phys, 2009;292(2):417-429.
- [4] A. Cibik, S. Kaya, A projection based stabilized finite element method for steady-state natural convection problem, J. Math. Anal. Appl, 2011;381(2):469-484.
- [5] Y.Z. Zhang, Y.R. Hou, H.E. Jia, Sub-grid stabilized defect-correction method for a steady-state natural convection problem, Comput. Math. Appl, 2014;67:497-514.
- [6] R.H. Nochetto, J.H. Pyo, The gauge-Uzawa finite element method II: The Boussinesq equations, Math. Models Methods Appl.Sci, 2006;16(10):1599-1626.
- [7] T. Zhong, Y.X. Qian, The time viscosity-splitting method for the Boussinesq problem, J. Math. Anal. Appl, 2017;445(1):186-211.
- [8] Y.Z. Zhang, Y.R. Hou, The Crank-Nicolson extrapolation stabilized finite element method for natural convection problem. Math Probl Eng, 2014;2:1-22.
- [9] Z.Y. Si, Y.N. He, K. Wang, A defect-correction method for unsteady conduction convection problems I: spatial discretization, Sci.China Math, 2011;54(1):185-204.
- [10] Z.Y. Si, Y.N. He, T. Zhang, A defect-correction method for unsteady conduction-convection problems II: time discretization. J. Comput. Appl. Math. 2012;236(9):2553-2573.
- [11] Z.Y. Si, Y.F. Lei, T. Zhang, Unconditional optimal error estimate of the projection/Lagrange-Galerkin finite element method for the Boussinesq equations, Numer. Algorithms, 2020;83(2):669-700.
- [12] H.X. Liang, T. Zhang, Stability and convergence of two-grid Crank-Nicolson extrapolation scheme for the time-dependent natural convection equations, Math.Methods Appl.Sci, 2019;42(18):6165-6191.

- [13] J.A. Fiordilino, A second order ensemble timestepping algorithm for natural convection, SIAM J. Numer. Anal., 2018;56(2):816-837.
- [14] O. Johansson, H. Kreiss. Über das Verfahren der zentralen Differenzen zur Lösung des Cauchy problems für partielle Differentialgleichungen, BIT Numerical Mathematics, 1963;3(2):97-107.
- [15] W. Layton and C. Trenchea. Stability of two IMEX methods, CNLF and BDF2-AB2, for uncoupling systems of evolution equations. Appl. Numer. Math., 2012;62(2):112-120.
- [16] M. Kubacki, Uncoupling evolutionary groundwater-surface water flows using the crank-Nicolson leapfrog method, Numer. Methods Partial Differ. Equ., 2013;29(4):1192-1216.
- [17] K. Michaela, M. Marina Analysis of a second-order, unconditionally stable, partitioned method for the evolutionary Stokes-Darcy model. Int. J. Numer. Anal. Model., 2015;12(4):704-730.
- [18] Q.L. Tang, Y.Q. Huang, Stability and convergence analysis of a Crank-Nicolson leap-frog scheme for the unsteady incompressible Navier-Stokes equations, Appl. Numer. Math, 2018;124:110-129.
- [19] J. Shen, On error estimates of the projection methods for the Navier-Stokes equations: second-order schemes, Math. Comp, 1996;65(215):1039-1065.
- [20] H.E. Jia, H.Y. Jia, Y.Q. Huang, A modified two-grid decoupling method for the mixed Navier-Stokes/Darcy model. Comput. Math. Appl, 2016;72(4):1142-1152.
- [21] Y.W. Guo, Y.N. He, Unconditional convergence and optimal L^2 error estimates of the Crank-Nicolson extrapolation FEM for the nonstationary Navier-Stokes equations, Comput. Math. Appl, 2018;75(1):134-152.
- [22] F. Hecht, New development in FreeFem++, J Numer Mat. 2012;20(3-4):251-265.
- [23] W.B. Chen, M. Gunburger, F. Hua, X.M. Wang, Efficient and long-time accurate second-order methods for Stokes-Darcy system, SIAM J Numer Anal, 2013;51(5):2563-2584
- [24] P. M. Gresho, R. L. Lee and S. T. Chan, Solution of the time-dependent incompressible Navier-Stokes and Boussinesq equations using the Galerkin finite element method[J], in Lecture Notes in Math. 1980;771: 203-222.
- [25] K. Onishi, T. Kuroki and N. Tosaka, Further development of BEM in thermal fluid dynamics[J], Develop. Bound. Elem. Meth. 1990;6: 319-345.
- [26] L. Q. Tang, T. H. Tsang, A least-squares finite element method for time-dependent incompressible flows with thermal convection, Int. J. Numer. Meth. Fluids, 1993;17: 271-289.